Remote sensing of atmospheric carbon monoxide with the MOPITT Airborne Test Radiometer (MATR)

Mark W. Smith*, Stephen R. Shertz, and Nuri Delen

Atmospheric Chemistry Division

National Center for Atmospheric Research

PO Box 3000, Boulder, CO 80307-3000

ABSTRACT

The MOPITT Airborne Test Radiometer (MATR) uses gas filter correlation radiometry to measure tropospheric carbon monoxide (CO) with three optical channels or methane (CH_4) with one channel. MATR uses the same gas correlation techniques as does the MOPITT satellite instrument, namely length modulation and pressure modulation. MATR data serves to test retrieval techniques for converting infrared radiometric data into atmospheric CO, or CH_4, amounts. MATR will also be applied to MOPITT data validation. This paper gives an overview of the MATR instrument design; it discusses the results of laboratory testing and calibration; and it presents results from recent flights.

Keywords: MATR, MOPITT, carbon monoxide, remote sensing, gas correlation, radiometry, infrared

1. INTRODUCTION

The MOPITT Airborne Test Radiometer (MATR) is a 3-channel gas filter correlation radiometer that supports the Measurements Of Pollutants In The Troposphere (MOPITT) satellite program. MOPITT will be launched on the EOS Terra platform and will measure tropospheric carbon monoxide (CO) profiles and methane (CH_4) columns.[1,2] MATR uses the same physical techniques as MOPITT (i.e., gas filter correlation radiometry with pressure modulation and length modulation) to remotely sense atmospheric CO, or CH_4, from an aircraft. MATR has two functions. The first function is to collect data to test our ability to retrieve correct atmospheric CO, or CH_4, gas amounts from MOPITT-like gas filter radiometer data. The second function is to help validate MOPITT data as described in the MOPITT data validation plan.[3] The MOPITT CO and CH_4 retrieval techniques have been described elsewhere.[4-6] CO and CH_4 are of scientific interest because of their roles as abundant fuels in the photochemical oxidation, or low temperature combustion, process that occurs in the troposphere.[7]

The basic measurement technique that is used by both MOPITT and MATR is remote sensing by means of infrared radiometry. The instruments measure infrared radiation (IR); gas concentrations in the atmosphere are inferred from the IR measurements. Fig. 1 depicts two fundamentally different types of atmospheric radiative transfer processes. In the first type of process, shown at left in Fig. 1, infrared radiation is emitted by the surface of the earth and then absorbed and partially re-emitted by the atmosphere. Because the atmosphere is in general colder than the surface of the earth, less radiation is re-emitted than is absorbed, resulting in net absorption. In the second type of process, shown at right in Fig. 1, infrared radiation is emitted by the sun and then partially absorbed by the atmosphere. Both processes can occur simultaneously. However, the first process is dominant for the CO fundamental absorption band near 4.6 micrometers, while the second process is dominant for the CO first overtone band near 2.3 micrometers, as well as for the methane bands near 2.2 micrometers.

2. INSTRUMENT DESIGN

MATR has been developed in stages, starting with a laboratory breadboard instrument that had only a 2.2/2.3 micrometer LMC channel. A flight prototype, again with only a 2.3/2.3 micrometer LMC channel, was then built. A few tests flights were made with this instrument in 1996.[8] The second generation flight instrument, with 3 optical channels, is described in this paper.

* Correspondence: Email: mwsmith@ncar.ucar.edu; Telephone: 303 497 1856; Fax: 303 497 1492

2.1 Optical Design

Fig. 2 shows the layout of the MATR optical table. As stated earlier, MATR has 3 optical channels. Channels 1 and 2 use a length modulated gas correlation cell (LMC) filled with CO. Channel 1 has a spectral pass band centered near 2.33 micrometers with a full width at half maximum (FWHM) of about 0.022 micrometers. It provides information about CO throughout an entire atmospheric column. Channel 2 has a spectral pass band centered near 4.61 micrometers with a FWHM of about 0.110 micrometers. It provides information about CO weighted in the mid-troposphere. Channel 3 has nominally the same spectral pass band as channel 2, but it uses a pressure modulated gas correlation cell (PMC) to provide information about CO weighted in the upper troposphere. By changing a band pass filter and the gas in the LMC, MATR can alternatively operate with a single channel centered near 2.27 micrometers to measure CH_4 column amounts.

A rotating input mirror selects one of four sources of input radiation: scene, cold blackbody, hot blackbody, or tungsten lamp. The last three sources are used for in-flight radiometric calibration. MATR collects scene data with a nominally nadir view, except when the aircraft is pitched up or down or is banking. The instrument full angle field of view (FOV) is approximately 5.7°, or 0.1 radians, producing a ground instantaneous FOV of about 1.2 km from the standard 12 km flight altitude.

The chopper produces an approximately square chopped waveform with a chopping frequency of about 400 Hz in normal operation. The data processing scheme uses only data acquired with the chopper fully open or fully closed, which comprises about 70% of the data.

Beam splitter 1 transmits most of the 2.2 to 2.3 micrometer radiation and about half of the 4.6 micrometer radiation to the LMC. It reflects about half of the 4.6 micrometer radiation towards the PMC. Beam splitter 2 transmits the 2.2 to 2.3 micrometer radiation to the channel 1 detector and reflects 4.6 micrometer radiation to the channel 2 detector.

The LMC is very similar to the version described in detail by Tolton and Drummond[9] and its operation will only be summarized here. The absorption path length for the correlation gas in the LMC is made to alternate between 2 mm and 10 mm by means of an internally rotating glass displacer. The displacer is a bow tie shaped piece of CaF_2 that is nearly transparent at the MATR operational wavelengths. The correlation gas in the LMC may be either CO or CH_4. The standard operating pressure is 80 kPa and the standard modulation frequency is 1/32 of the chopping frequency.

The PMC was built by the University of Oxford and is similar to the MOPITT flight PMCs. Again, the operation of a PMC has been described in detail elsewhere[10,11] and will only be summarized here. A pair of pistons changes the volume of a gas reservoir and this causes the pressure of the correlation gas in the PMC optical cell to oscillate from about 5 to 11 kPa at 1/8 of the chopping frequency.

The LMC and the PMC provide extremely high resolution spectral filtering. This resolution is on the order of the widths of the gas lines in the cells, or roughly 0.1 to 1 nm, depending on cell conditions. Additional low resolution filters are required to set the overall optical pass band for each channel. These filters limit detector response to spectral regions in which the correlation gas has strong absorption features. A pair of filters set the spectral pass band of each optical channel in MATR. The actual spectral pass band for each channel is set by a narrow filter that is located external to each detector Dewar. These filters are located where the optical beam is nearly collimated, so as to minimize angle of incidence effects on the filter. A second filter, with a moderately broad pass band, is located in each Dewar. This filter is cooled to liquid nitrogen temperature and blocks most of the thermal background radiation. Radiation is converging rapidly on to the detector element in each Dewar, and this produces an inevitable shift in the pass band of the filters in the Dewars. However, this shift has no real impact on the ability of the cooled filter to block thermal background radiation.

The MATR infrared detectors each use a single 4 mm diameter InSb element that is cooled by liquid nitrogen in a Dewar. The detector elements operate in photo-voltaic mode with a matched transimpedance pre-amplifier. The input FET's and first stage feedback resistors for each pre-amplifier are mounted on a cold finger inside each Dewar to minimize Johnson noise from the feedback resistors. DC-coupled outputs from the detectors are used to check for saturation. AC-coupled outputs are amplified and filtered and then used as the primary radiometric signals.

2.2 In-flight Radiometric Calibration Assembly

In-flight radiometric calibration is accomplished with the use of three calibration sources. A pair of blackbodies, one heated to about 40 °C and one cooled to about 2 °C, is used to derive radiometric gain and offset coefficients for the 4.6 micrometer channels. A thin sheet of Spectralon diffusing material that is illuminated by a quartz tungsten halogen (QTH) lamp is used as a source for the 2.3 micrometer channel. The blackbody temperatures as well as the supply voltage and current for the QTH lamp are monitored and recorded in normal operation. The in-flight blackbodies are calibrated in the laboratory against a reference blackbody that has been calibrated directly by NIST. The in-flight QTH source is calibrated against a set of QTH lamps that were purchased from a vendor; the vendor supplied reports that trace lamp calibration to NIST reference standards.

2.3 Thermal Control

The optical table is completely enclosed in a foam insulated box. The interior of the box is stabilized at about 32 °C by a combination of convective and conductive heating. A heat pump removes the power that is generated from the chopper motor, which is the only appreciable heat source on the optical table. Temperatures are monitored and recorded for 16 points throughout the instrument, in addition to the blackbodies.

2.4 Auxiliary Instrumentation

Post-flight data analysis requires auxiliary information in addition to the detector outputs and instrument temperatures. A global positioning system (GPS) provides latitude, longitude and geometrical altitude. Ambient pressure at flight altitude, as determined by an aircraft altimeter, is also recorded. A position and orientation system provides aircraft attitude data. When interpreting the radiometric data, it is useful to know if the scene was clear or cloudy, water or land, vegetated or bare, simple or complex, etc. This information is provided by a nadir-viewing video camera that has a full-angle FOV of 14.4°, which is about 2.5 times greater than MATR's FOV.

2.5 Instrument Control and Data Acquisition

Instrument control and data acquisition are performed by an industrial grade rack mounted computer that contains five data acquisition boards: two general purpose A/D and digital I/O boards, one counter/timer board, and a pair of dual-port RS-232 boards. The computer has a 133 MHz 586 CPU and a 6 GByte hard drive. A backup copy of data is written in real time onto a 1 Gbyte removable media Jaz disk, which can hold about 8 hours worth of data. These large capacity removable disks provide a convenient means of transferring data to other platforms for post-flight processing.

All data acquisition software has been developed using National Instrument's LabWindows/CVI and NiDAQ software. The main source code is written in ANSI C, with frequent calls to National Instruments' library functions. All user interaction is handled through graphical user interface (GUI) display panels. The code is compiled into a standalone executable file. The software features numerous real time displays that allow all of the instrument outputs to be viewed either as low level (i.e., unprocessed) values or as numerically processed values. This has been useful to monitor the instrument for correct operation in-flight, as well as to diagnose problems when they occur.

2.6 Size, Weight and Power

The overall size of the MATR optical table is 41 cm wide by 67 cm long by 39 cm high, including thermal and electrical controls, but not including the in-flight radiometric calibration assembly. Additional electronics and the video recorder occupy about 24" in height in a standard 19" wide electronics rack. The position and orientation system uses another 7" of rack height. The power supply electronics use as input 28 V DC and 110 V AC electrical power that is supplied by the aircraft. Total power consumption is somewhat less than 1400 W (50 A) at 28 V DC and less than 330 W (3 A) at 110 V AC. Power for the detectors' pre-amplifiers is provided by a pair of nominally 12 V re-chargeable lead acid storage batteries, for minimum electrical noise. An un-interruptible power supply (UPS) with 110 V AC output ensures power integrity to the computer.

2.7 Aircraft

MATR has been flown in a Cessna Citation II aircraft that is owned by the Department of Energy and operated out of the Remote Sensing Laboratory in Las Vegas, Nevada. The service ceiling for the aircraft is 13 km, but in practice a cruise altitude of 12 km has been used for MATR deployments. The standard cruise speed at 12 km altitude is about 660 km/hr. The flight range (until 30 minute reserve) is about 2,400 km.

3. LAB TESTING AND CALIBRATION

A variety of tests and calibrations have been carried out for MATR. These include the following: calibration of temperature, pressure, and other engineering transducers; tests to establish the timing of the gas modulations and chopping with respect to the data acquisition timing; linearity tests; gain setting tests; scan mirror repeatability tests; checks for total out-of-field (stray light) response; characterization of the effect of chopper blade temperature on radiometric response; radiometric calibration; tests of signal-to-noise ratio with a stable radiance source; tests of the LMC behavior as a function of fill pressure; tests of the PMC pressure cycle. This paper will present in detail the results of only a few of the most significant tests and calibrations.

3.1 Detector Output Waveforms and Instrument Timing

In order to process the gas correlation data from MATR, it is necessary first to establish the timing of the gas modulations and chopping with respect to the data acquisition. The LMC, PMC and chopper are all phase locked to reference frequencies that are derived from a single master clock, which is also tied to the data acquisition timing. The data acquisition trigger is derived from the actual phases of the modulators as determined from optical encoders. The first chopper transition that follows an LMC short-to-long path transition triggers a data acquisition sequence. Data is then acquired for a period of time that corresponds to 5 LMC states, which equals 5 PMC cycles.

Fig. 3 shows the AC-coupled output of the channel 2 detector (4.6 micrometer LMC channel). The chopper produces the high speed, nearly square wave chopping. The amplitude of this square wave is proportional to the difference between the chopper blade radiance and the input source radiance, as observed through the LMC. The overall modulation envelope is produced by the LMC. The low, flat portions of the envelope correspond to strong absorption by the 10-mm gas path (CaF_2 displacer is out of the beam). The high, flat portions correspond to weaker absorption by the 2-mm gas path (CaF_2 displacer is in the beam). The sloping portions occur when the edge of the CaF_2 displacer is moving through the beam. As mentioned before, the only data retained for processing is that acquired with the chopper fully open or fully closed, and with the displacer completely in the beam or completely out. The data shown in Fig. 3 is used to determine when these conditions are true.

Fig. 4 shows how the high resolution spectral filtering of a gas correlation device is derived. In this idealized case, 3 gas absorption lines are present within the pass band of the channel filter. The thin dashed line at top shows transmittance through the gas and band pass filter with a small amount of gas in the correlation cell. This state corresponds to the intervals from 0.02 to 0.03 s and from 0.06 to 0.07 s in Fig. 3. The other thin dashed line shows transmittance with a large amount of gas in the correlation cell. This corresponds to the intervals from 0.0 to 0.01 s, from 0.04 to 0.05 s, and from 0.08 to 0.09 s in Fig. 3. One can numerically convert the chopped signal amplitudes for these two states into average and difference signal amplitudes. These average and difference signal amplitudes then correspond to two distinct spectral response functions. The average spectral response function, shown as a heavy solid line in Fig. 4, is very close to the transmittance of the band pass filter, with slight dips at the gas absorption wavelengths. The difference spectral response function, shown as a thin solid line in Fig. 4, peaks only at wavelengths where the gas in the correlation cell absorbs.

Fig. 5 shows the AC-coupled output of the channel 3 detector (4.6 micrometer PMC channel). The high frequency modulation of the chopper is still evident. However, the modulation envelope produced by the PMC has a sinusoidal character due to the more or less sinusoidal variation of pressure in the PMC. For the PMC, data is again considered valid only when the high frequency chopper is fully opened or fully closed. However, a two term Fourier expansion is used to describe the PMC modulation envelope.

3.2 Spectral characterization

Knowledge of the instrument's spectral response functions, illustrated in idealized form in Fig. 4, is important for analysis of many of the tests and calibrations, and is especially important for carrying out retrievals of atmospheric CO, or CH_4. The spectral response functions can be separated into two components: the first is the transmittance of the gas in the correlation cell for each channel; the second is the transmittance of the band pass filter in each channel. As the spectral parameters of CO (i.e., line positions, line strengths, and pressure broadening coefficients) have been measured with very good precision and accuracy,[12] it is possible to calculate with sufficient precision and accuracy the transmittance of the gas in the correlation cells, provided we detemine with sufficient precision and accuracy the path length, temperature, and pressure for each state of each correlation cell.

For the transmittance of the band pass filters, we originally used the transmittance curves that were supplied by the filter manufacturers. We also had the transmittance of one of the 4.6 micrometer filters measured by colleagues at the University of Toronto, using a Fourier transform spectrometer. The results of the two different characterizations are shown in Fig. 6. There is a shift of approximately 0.006 nm between the two results. This shift has not been very significant when interpreting laboratory tests, and the manufacturer's filter profile was used to analyze the results presented in sections 3.3 and 3.4. However, the filter shift has been very significant for retrievals of atmospheric CO, and this will be discussed in sections 4.1 and 5.

3.3 LMC Modulation Tests

For this paper, LMC modulation is defined as the ratio of the LMC difference signal radiance to the LMC average signal radiance, or R(D/A). Fig. 7 shows measured and calculated values of R(D/A) for the 2.3 micrometer LMC channel for CO fill pressures from 0 to 90 kPa (measurements) or 100 kPa (calculations only). Best fit lines are also shown. The best fit slopes for the measurements and calculations agree to within about 0.3%. Ideally the intercept values should be zero. The intercept for the calculations is non-zero and slightly negative (i.e., -5.2×10^{-6}) because R(D/A) is not a strictly linear function of LMC fill pressure. The intercept for the measurements is non-zero and slightly positive (i.e., 4.2×10^{-6}). The intercept for the measurements is influenced by the slight non-linearity in R(D/A) as well as by the slight modulation that is produced by the CaF_2 displacer. This spurious modulation has also been called the LMC imbalance.[9]

Fig. 8 shows measured and calculated values of R(D/A) for the 4.6 micrometer LMC channel for CO fill pressures from 0 to 80 kPa. Values for views of the hot blackbody (HBB) at 40 °C and of the cold blackbody (CBB) at 2 °C are plotted. Measured values are shown as discreet markers (filled circles for the HBB and open circles for the CBB). Calculated values are plotted as lines (solid for the HBB and dashed for the CBB). Because the absorption by the fundamental band at 4.6 micrometers is so much stronger than absorption by the first harmonic band at 2.3 micrometers, R(D/A) at 4.6 micrometers is not an especially linear function of CO fill pressure, and so best fit lines are not shown. The calculated values for the HBB and CBB are in fact identical. The measured values for viewing the HBB agree with the calculated values to within 0.7% at 80 kPa, while for the CBB the agreement is about 2.7%. For the HBB, the agreement between the measured and calculated values is about the same for all fill pressures. However, the measured and calculated values for the CBB converge at the mid-point, or 40 kPa, and then diverge at lower and higher fill pressures. This indicates that some unknown source of instrument error is present when viewing the CBB. Inspection of the average and difference radiance signals shows that almost all of the error is associated with the difference signal. However, the source of the error has not yet been identified.

3.4 PMC pressure cycle tests

Fig. 9 shows measured and calculated values of the PMC pressure cycle. The calculations were performed using a model that was originally developed to describe PMCs that were carried aboard the ISAMS satellite.[13] After adjustments were made to various model parameters, the model was able to do a good job of predicting the maximum and minimum pressures in the PMC. However, the measured pressure has a more rapid decrease from the maximum and a less rapid increase from the minimum than does the calculated pressure. Alternatively one could say that the measured pressure has a slight phase lead when the expansion portion of the cycle begins, and a slight phase lag when the compression portion of the cycle begins. Although only pressure is plotted, the model calculates both the pressure and the temperature of the gas in the PMC. Both pressure and temperature are required to calculate the transmittance of the correlation gas in the PMC.

4. FLIGHT RESULTS

MATR was put through a set of flights in February and March, 1998. The instrument functioned with no outright failures, but several problems were noted. In particular, some thermal control problems were discovered and addressed. In addition, a leak in the LMC was noted and fixed. Another set of flights were made in January and February, 1999. CO retrievals from two of these flights are shown in Figs. 10 and 11. The retrievals used only the 4.6 micrometer LMC (channel 2) data. The retrieval process used is relatively straightforward. A forward model is used to calculate atmospheric radiance values, starting with an assumed surface emissivity of 0.98, with water vapor and temperature profiles obtained from nearby radio sondes, with CO values set initially to 100 ppbv mixing ratio at all altitudes, and with fixed profiles for other absorbing species. Surface temperature is then adjusted until the calculated average signal radiance agrees with the measured average signal radiance. The CO mixing ratio is then adjusted until the calculated difference signal radiance agrees with the measured difference signal radiance. A final iteration is then made to the surface temperature.

4.1 Flight results over Carr, Colorado

Fig. 10 shows CO values that were retrieved from MATR measurements made over Carr, Colorado on 4 Feb. 1999. On this day in situ measurements, made by a group from the NOAA Climate and Monitoring Diagnostics Laboratory, were also available. A CO mixing ratio of 80 ppbv was retrieved when the manufacturer's filter profile was used. A CO mixing ratio of 155 ppbv was retrieved when the University of Toronto filter profile was used. Compared to the in situ results, the value retrieved using the manufacturer's filter profile is too low, while the the value retrieved using the manufacturer's filter profile is too high.

4.2 Flight results over Los Angeles and Pacific Ocean

Fig. 11 shows CO values that were retrieved from MATR measurements made over Los Angeles and the nearby Pacific Ocean on 22 Jan. 1999. Only results obtained using the manufacturer's filter profile are shown. On this day fairly strong winds were blowing from the west to the east, and so the air over the Pacific could be considered "unpolluted". The average value over the ocean is 56 ppbv, and the concentrations over Los Angeles peak near 200 ppb. Based on the results obtained over Carr, Colorado, these values are probably too low. However, Fig. 11 clearly shows a strong instrumental response when going from a region where low and constant CO values are expected (i.e., the Pacific Ocean) to a region where high and variable CO values are expected (i.e., the Los Angeles basin). The standard deviation of the measurements over the Pacific is 3.8 ppbv, with a time period for signal averaging that corresponds to about 2.5 km of distance traveled by the Citation aircraft. Even if this standard deviation were doubled (based on the different results over Carr for the different filter profiles), the precision is well within the target of 10 ppbv. Furthermore, this is with spatial resolution of 1.2 km (across the flight track) by 2.5 km (along the flight track), which is quite small compared to the MOPITT pixel size of about 22 km by 22 km.

5. Summary and Discussion

MATR was conceived for two functions: first to collect data to test our ability to retrieve correct atmospheric CO, or CH_4, gas amounts from MOPITT-like gas filter radiometer data; and second to help validate MOPITT data. The instrument has been designed, built, and flown to collect data. The retrieval results from recent flights strongly suggest the need to calibrate carefully the spectral response of the band pass filters in each channel. Although two different measurements were made of the band pass filters for the 4.6 micrometer channels, the results differ, and there is no clear criteria for deciding which, if either, result is correct. Furthermore, these measurements were made on the band pass filters alone. Although the transmittance of the rest of the optics is not expected to vary strongly with wavelength, a true end-to-end calibration of the entire MATR instrument should be preformed. A monochromator system has been assembled for this purpose and these measurements are planned for the near future. There is also a need to understand the anomalous behavior of the LMC thermal channel when looking at the cold blackbody source. There is also a need to obtain additional data to compare MATR retrieval results to in situ measurements, as a single day is really insufficient to demonstrate valid instrument performance. Additional flights to obtain this data are scheduled for August, 1999. Finally, additional work needs to be done to make use of the channel 1 (2.3 micrometer LMC) and channel 3 (4.6 micrometer PMC) data. This work is under way.

ACKNOWLEDGMENTS

The MATR project is funded by NASA under contract NAS5-30888 administered through Dr. Michael King's office and this funding is gratefully acknowledged. John Gille supervises the MATR project. Kate Paulin made the calculations of PMC pressure cycle that are shown in Fig. 9.

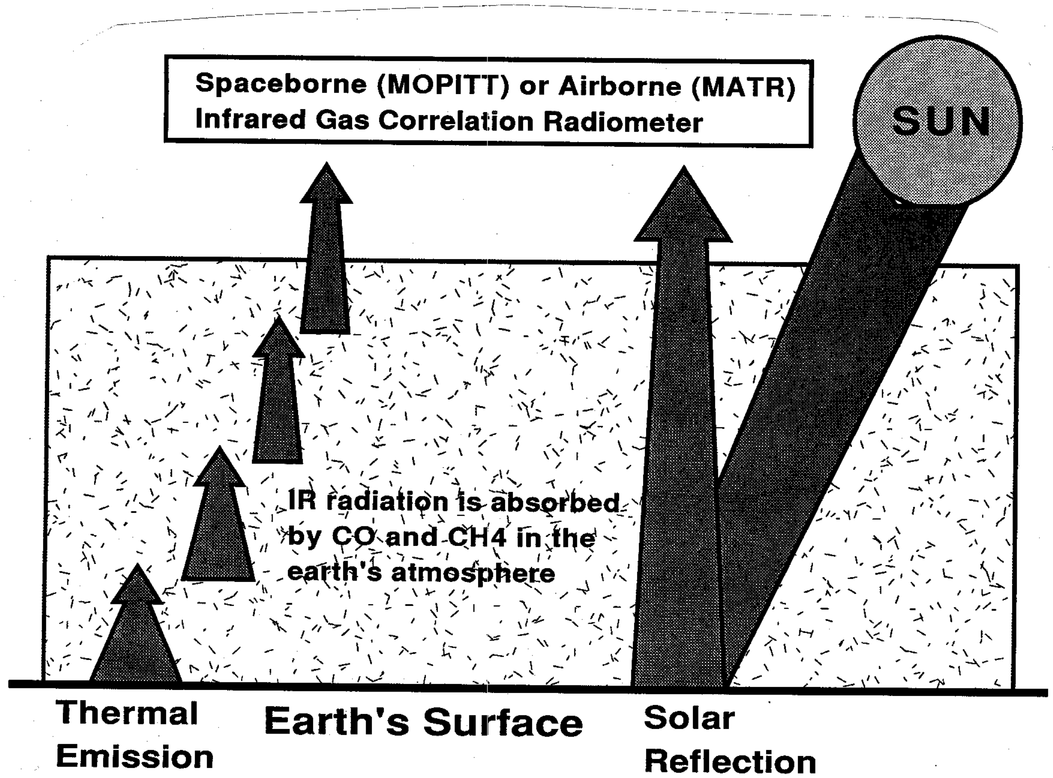

Figure 1. Schematic illustration of atmospheric radiative transfer and remote sensing processes.

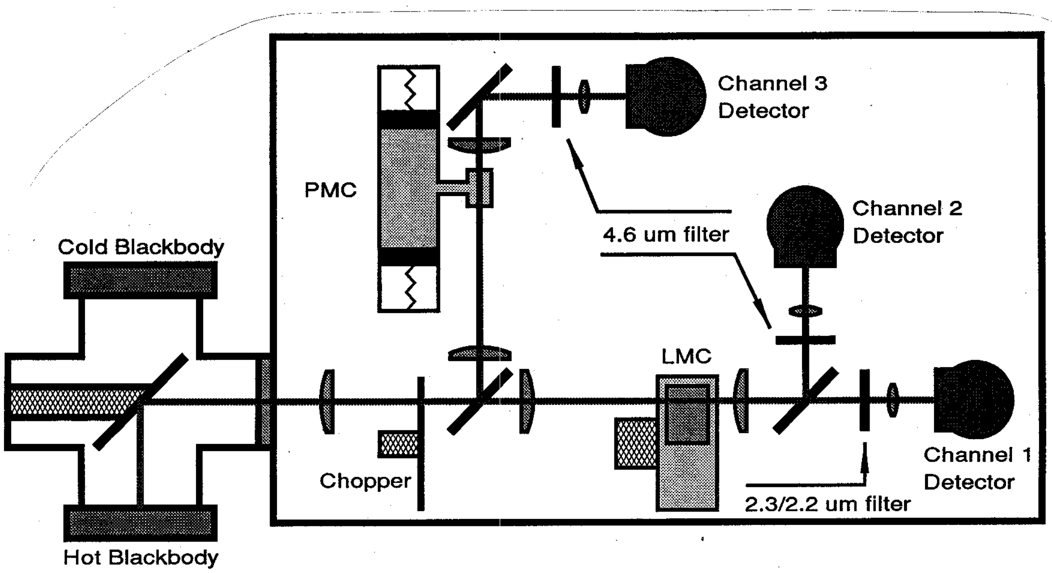

Figure 2. MATR optical table.

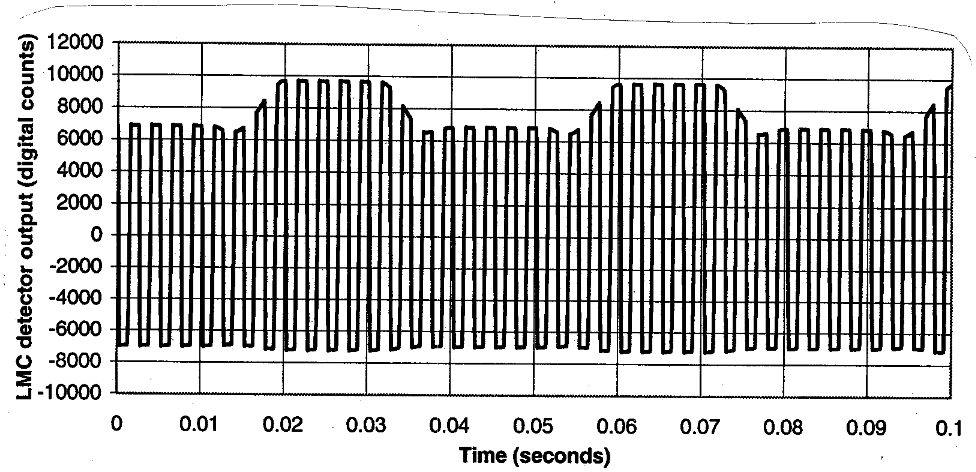

Figure 3. AC-coupled detector signal for MATR 4.6 micrometer LMC channel.

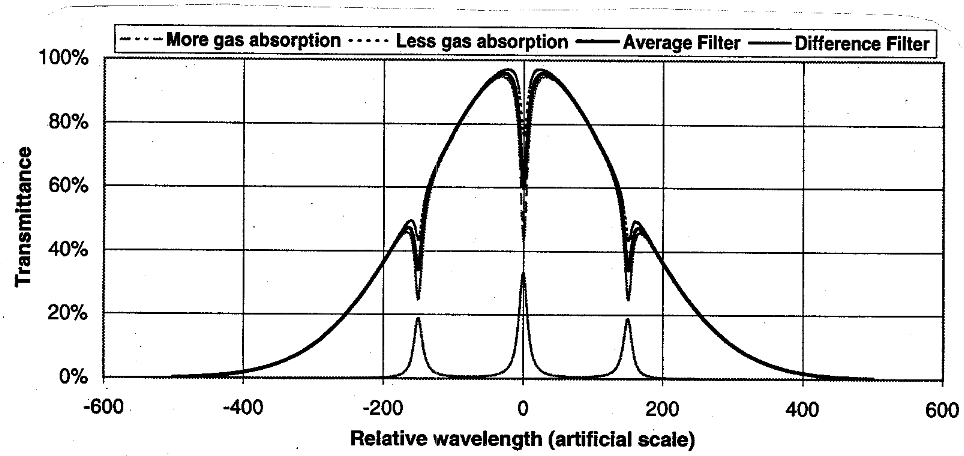

Figure 4. Idealized spectral response functions for a gas correlation filter radiometer.

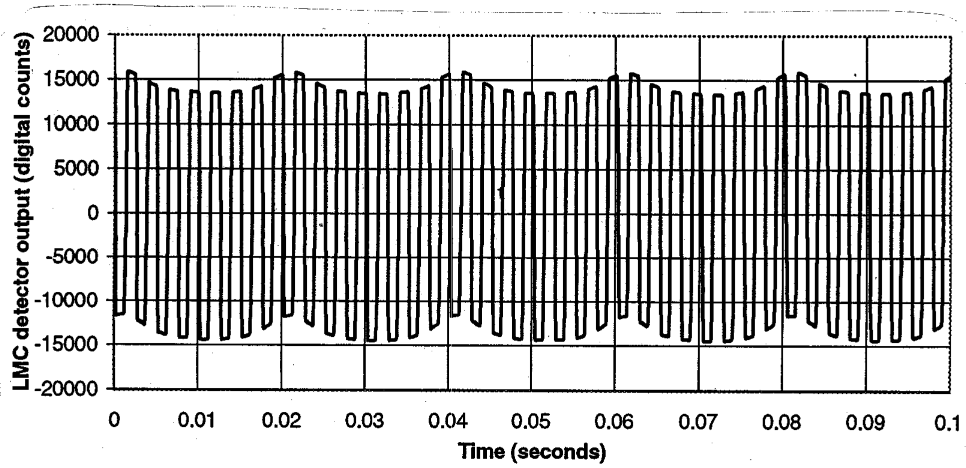

Figure 5.. AC-coupled detector signal for MATR 4.6 micrometer PMC channel.

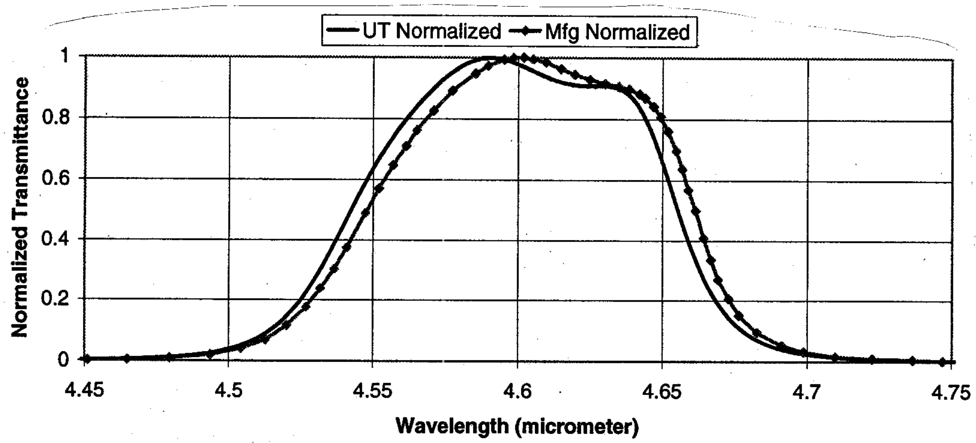

Figure 6. Spectral pass band for 4.6 micrometer channels as determined by filter manufacturer and University of Toronto.

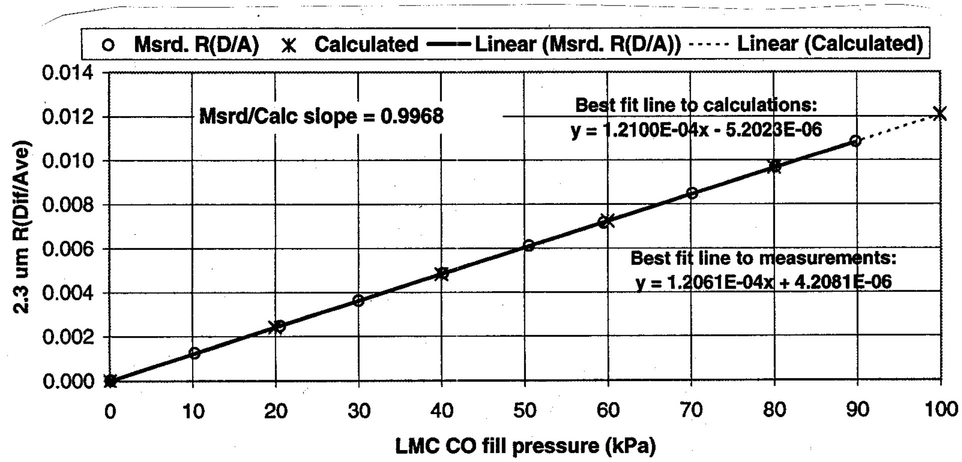

Figure 7. Ratio(Dif/Ave) as a function of LMC fill pressure for 2.3 micrometer channel.

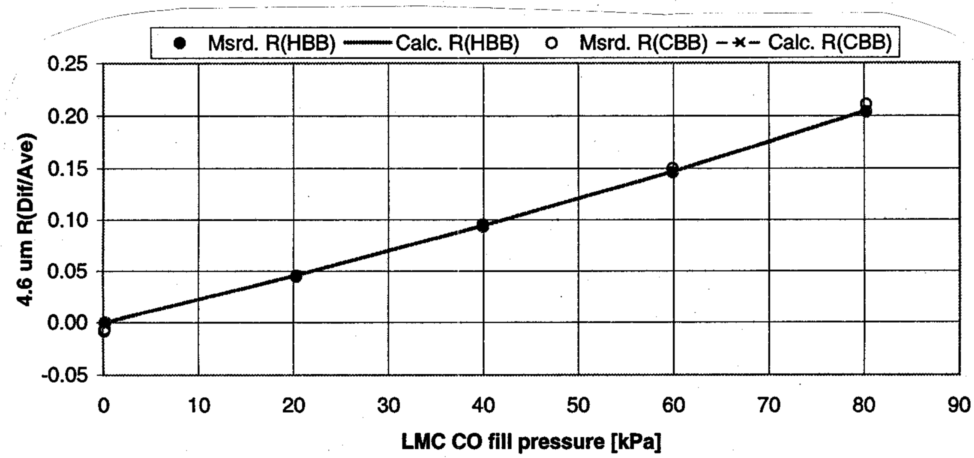

Figure 8. Ratio(Dif/Ave) as a function of LMC fill pressure for 4.6 micrometer channel.

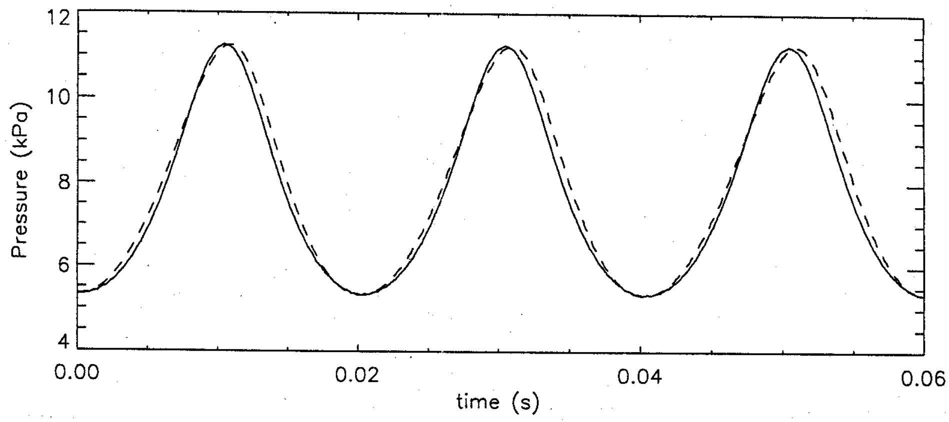

Figure 9 Calculated (dashed line) and measured (solid line) PMC pressure cycles.

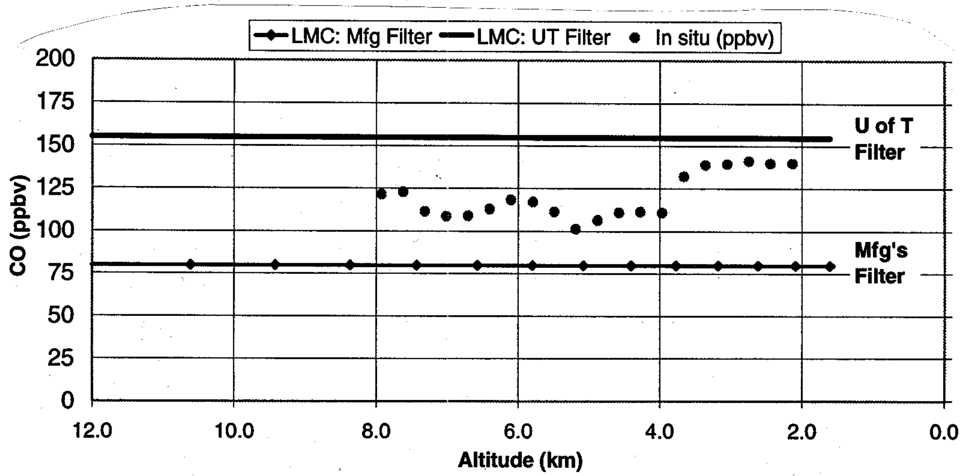

Figure 10. CO values from in-situ measurements and MATR retrievals over Carr, CO on 4 Feb. 1999 for both filter profiles

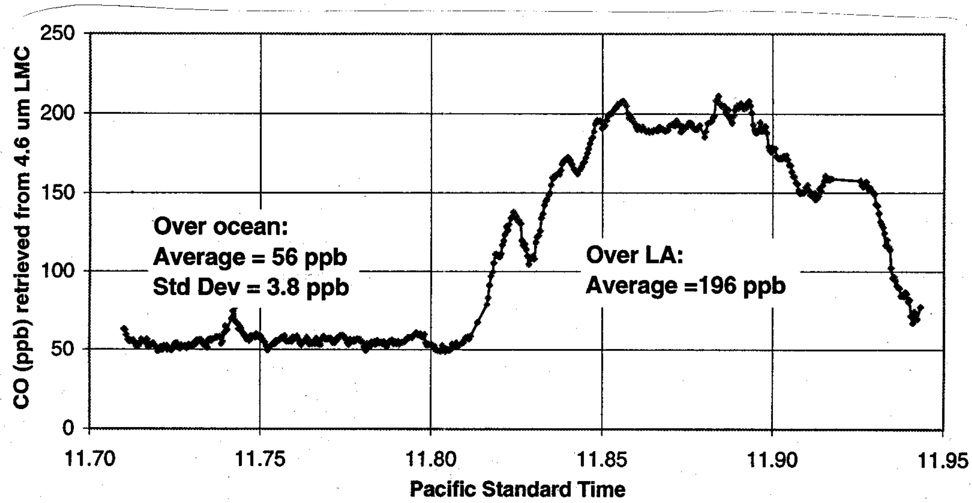

Figure 11. CO retrieved from MATR data over Los Angeles and Pacific on 22 Jan. 1999 using manufacturer's filter profile.

REFERENCES

1. J.R. Drummond, "Measurements of Pollution in the Troposphere (MOPITT)," in *The Use of EOS for Studies of Atmospheric Physics*, J.C. Gille and G. Visconti, Eds., pp. 77-101, North-Holland, Amsterdam (1992).

2. J.R. Drummond, G.P. Brasseur, G.R. Davis, J.C. Gille, J.C. McConnell, G.D. Peskett, H.G. Reichle, Jr., and N. Roulet, "MOPITT Mission Description Document," Department of Physics, University of Toronto, Toronto, Canada (Oct. 1996). Available HTTP: http://www.atmosp.physics.utoronto.ca Directory: /Research Groups/MOPITT

3. J. Wang, J. Gille, P. Bailey, M. Smith, L. Pan, D. Edwards, L. Rokke, J. Drummond, G. Davis, H. Reichle, "MOPITT Data Validation Plan," National Center for Atmospheric Research, Boulder, Colo. (Sept. 1996). Available HTTP: http://eos.acd.ucar.edu Directory: /mopitt/val_plans.html File: Version 3 validation plan (in various formats).

4. L. Pan, J.C. Gille, D.P. Edwards, P.L. Bailey, "Retrieval of tropospheric carbon monoxide for the MOPITT experiment," *J. Geophys. Res.*, **103** (D24), pp. 32,277-32,290 (Dec. 1998).

5. L. Pan, J.C. Gille, C.D. Rodgers, D.P. Edwards, P.L. Bailey, L.A. Rokke, J. Wang, "Analysis and characterization of the retrieval algorithm for measuring tropospheric CO using the MOPITT instrument," *Proc. of SPIE*, **2830**, pp. 159-168 (Aug. 1996).

6. NCAR MOPITT Team, "MOPITT: Algorithm Theoretical Basis Document," National Center for Atmospheric Research, Boulder, Colo. (July 1995). Available HTTP: http://eos.acd.ucar.edu Directory: /mopitt/atbds.html File: Level-2 ATBD (in various formats).

7. J.H. Seinfeld, S.N. Pandis, *Atmospheric Chemistry and Physics*, Chapter 5, John Wiley & Sons, New York (1998).

8. M.W. Smith and S. R. Shertz, "Current plans and status of MOPITT Algorithm Test Radiometer (MATR)," *Proc. of SPIE*, **2820**, pp. 78-86 (Aug. 1996).

9. B.T. Tolton and J.R. Drummond, "Characterization of the length-modulated radiometer," *Appl. Opt.*, **36** (22), pp. 5409-5420 (Aug. 1997).

10. J.T. Houghton, F.W. Taylor, and C.D. Rodgers, *Remote Sounding of Atmospheres*, pp. 93-107, Cambridge University Press, Cambridge (1984).

11. F.W. Taylor, "Pressure Modulator Radiometry," in *Spectrometric Techniques, Vol. III*, G. A. Vanasse, Ed., pp. 137-196, Academic Press, New York (1983).

12. L.S. Rothman, R.R. Gamache, R.H. Tipping, C.P. Rinsland, M.A.H. Smith, D. Chris Benner, V. Malathy Devi, J.-M. Flaud, C. Camy-Peyret, A. Perrin, A. Goldman, S.T. Massie, L.R. Brown, and R.A. Toth, "The HITRAN molecular database: editions of 1991 and 1992," *J. Quant. Spectosc. Radiat. Transfer*, **48**, 5/6, pp. 469-507 (1992).

13. P. Venters, "The ISAMS PMC model," ISAMS document SW304, Oxford University (1991).